COMMUNICATIONS IN NUMERICAL METHODS IN ENGINEERING, Vol. 12, 303–316 (1996)

ONE-DIMENSIONAL STRETCHING FUNCTIONS FOR C^n PATCHED GRIDS, AND ASSOCIATED TRUNCATION ERRORS IN FINITE-DIFFERENCE CALCULATIONS

LUDWIG C. NITSCHE

Department of Chemical Engineering, The University of Illinois at Chicago, 810 South Clinton Street, Chicago, IL 60607, U.S.A.

SUMMARY

In this work the truncation-error criteria of Thompson and Mastin (1985) are combined with conditions of vanishing second and higher derivatives at both endpoints for the purpose of deriving new classes of one-dimensional stretching functions for mesh refinement in finite-difference numerics. With these elementary stretching functions, matching of the slopes between adjacent grid patches then automatically confers C^n regularity upon the composite stretching function. Formulated with reference to two conceptions of truncation order (fixed relative distribution against fixed number of nodes) the resulting mappings are shown to provide particularly advantageous node distributions at both ends simultaneously (with concomitantly higher truncation error in between). Viewed overall, the truncation-error functions compare favourably with those for sinh, tanh and erf – mappings whose utility for mesh refinement was established by Thompson and Mastin. The numerical labour of implementing the new stretching functions is only slightly greater than that required for the error function. An illustrative derivation involving C^n patching leads to two-sided stretching functions, which allow the slopes at both ends to be prescribed arbitrarily. This formulation differs from a previous approach described by Vinokur (1983).

KEY WORDS stretching functions; mesh refinement; finite differences; truncation error; composite grids; regularity

INTRODUCTION

In algebraically or elliptically generated grids for finite-difference calculations, local mesh refinement is carried out with stretching functions, whereby an evenly spaced set of points in an auxiliary (transformed) co-ordinate ξ is mapped into the desired non-uniform distribution in the physical-space co-ordinate x. For boundary-fitted grids, such a transformation may be compounded upon the curvilinear co-ordinates, or else be incorporated into the control functions themselves.[1,2]

Two main considerations govern the choice of stretching functions. Firstly, the mesh spacing should not vary too rapidly between coarse and fine portions of the mesh.[1–5] Secondly, in the case of composite or patched grids, continuity of the lineal density of grid points (and of at least some of its derivatives) is desirable, especially where the solution exhibits high curvature or other rapid spatial variations.[1,4,6] (The aim is to be able to carry the finite differences across the intervening 'artificial boundary'[1] without treating the associated nodes differently from any other interior grid points.[4]) Both aspects are motivated by truncation errors in the finite-difference representation of derivatives,[1–3,5,7–9] for which specific criteria regarding the

CCC 1069–8299/96/050303–14

Received 18 January 1994
Revised 27 November 1995

transition between different mesh densities have been formulated[1-3,9] that allow the evaluation of prospective choices of stretching functions.

Thompson and Mastin[3] (see also the monograph[2]) systematized the concepts of truncation order (variable number of points with fixed relative distribution against variable distribution with fixed number), and provided a catalogue of useful stretching functions. Perhaps most importantly, they quantified the relative merits of these functions using specific criteria that bear on truncation error. Generally, a tradeoff exists between desirably slow variation of spacing within the boundary layer against adequately high mesh density outside the boundary layer. Of the three most suitable stretching functions (constructed from the hyperbolic sine, hyperbolic tangent and error function) the first provides a more advantageous mesh distribution within the boundary layer while the latter two are better for the outer region. In these examples the 'better' end of the stretching function happens to be that at which the second derivative vanishes, a fact that is relevant to the developments below.

Complex gridding problems (e.g. in three-dimensional domains) can require the generality of interpolation methods[10,11] and/or adaptive refinement.[5] However, the simplest approach to certain cases involving multiple refinement/expansion zones would be to piece together several of the elementary stretching functions described above to obtain a composite stretching function with the desired undulations. (This approach will be related to more complicated, globally-defined functional forms.[12,1]) In this endeavour one is faced with a problem: although slopes can always be matched at the junctions,[9] the elementary stretching functions do not seem to admit any similarly straightforward scheme for matching higher derivatives. Thus, the purpose of this paper is to introduce new stretching functions that are readily conducive to splicing together with prescribed higher regularity at the matching points.

This paper proceeds from the following two premises. Firstly, the truncation-error criteria of Thompson and Mastin[3] can be applied *in reverse*, as a means of determining desirable stretching functions. Secondly, in order to match adjoining nth derivatives it is sufficient that the nth derivative of the stretching-function 'building blocks' vanish at both ends, a requirement that will turn out to be easy to incorporate. The latter aspect is also particularly useful for patching a boundary-layer mesh-refinement zone onto an evenly spaced grid.[1,12] These two ideas will be shown to have a fortunate confluence: the resulting stretching functions also turn out to exhibit the advantages of sinh within the boundary layer and of tanh or (even better) erf outside.

THE TRUNCATION-ERROR CRITERIA OF THOMPSON AND MASTIN

As the basis for subsequent arguments, we summarize here relevant elements from the work of Thompson and Mastin[3] (with minor changes in basis and notation); see also Chapter V in the monograph by Thompson, Warsi and Mastin.[2] Consider a uniform, one-dimensional mesh in the auxiliary co-ordinate ($0 \leq \xi \leq 1$),

$$\xi_i = i/N, \qquad i = 0, 1, 2, \ldots, N \tag{1}$$

which is mapped into a non-uniform mesh in the physical-space co-ordinate, $\{x_i\}$, by a stretching transformation

$$x = g(\xi), \qquad g(0) = 0, \qquad g(1) = 1 \tag{2}$$

For the central difference approximation of the slope,

$$\left(\frac{\mathrm{d}f}{\mathrm{d}x}\right)_i = \frac{N/2}{g'(\xi_i)}\,[f_{i+1} - f_{i-1}] + T_x \tag{3}$$

Thompson and Mastin expressed the truncation error T_x as a series in inverse powers of N^2, which could be truncated after the leading term to obtain the approximation

$$T_x \approx -\frac{1}{N^2}\left[\frac{1}{6}\,\frac{g'''(\xi)}{g'(\xi)}\,\frac{\mathrm{d}f}{\mathrm{d}x} + \frac{1}{2}\,g''(\xi)\,\frac{\mathrm{d}^2 f}{\mathrm{d}x^2} + \frac{1}{6}\,[g'(\xi)]^2\,\frac{\mathrm{d}^3 f}{\mathrm{d}x^3}\right] \tag{4}$$

Identifying the first two terms with non-uniformity of the grid, they arrived at the desired smallness of the functions

$$L_N^{(2)}(\xi) = g''(\xi)/g'(\xi), \qquad L_N^{(3)}(\xi) = g'''(\xi)/g'(\xi) \tag{5}$$

which served as criteria for the comparison of different stretching transformations in the limit as $\min_{0 \leq \xi \leq 1}\{g'(\xi)\} \to 0$.

An analogous derivation for the truncation order with a fixed number of grid points led to the (usually more stringent) truncation-error functions

$$L_S^{(2)} = g''(\xi)/[g'(\xi)]^2, \qquad L_S^{(3)} = g'''(\xi)/[g'(\xi)]^3 \tag{6}$$

Thompson and Mastin established that boundedness of these quantities (and of all higher-order versions) as $g'(\xi) \to 0$ was sufficient for truncation of the relevant series representation of the finite-difference truncation error.

On the basis of truncation error, Thompson, Warsi and Mastin[2,3] concluded that the metrical coefficient $g'(\xi_i)$ in (3) should be approximated with the same finite-difference formula, hence

$$\left(\frac{\mathrm{d}f}{\mathrm{d}x}\right)_i \approx \frac{f_{i+1} - f_{i-1}}{x_{i+1} - x_{i-1}} \tag{7}$$

In other words, for the first derivative one can ignore the non-uniformity of a grid and use the usual central-difference formula for equally-spaced points – provided that the grid spacing does not change 'too rapidly', as quantified by the truncation-error functions (5) and/or (6).

STRETCHING FUNCTIONS BASED UPON $L_N^{(2)}$

Here we specify the functional form of the truncation-error function $L_N^{(2)}$, (5), and deduce from this what the corresponding stretching function $g(\xi)$ must be. This task is facilitated by the observation that

$$g(\xi; A) = g'(0)\int_0^{\xi} e^{A\phi(t)}\,\mathrm{d}t \qquad \Rightarrow \qquad L_N^{(2)}(\xi; A) = A\phi'(\xi) \tag{8}$$

Indeed, one of the standard stretching functions[2,3] can be rewritten in this form, namely

$$\phi_1(\xi) = (2\xi - \xi^2) \qquad \Rightarrow \qquad g_1(\xi; A_1) = 1 - \frac{\mathrm{erf}[(1-\xi)\sqrt{A_1}]}{\mathrm{erf}(\sqrt{A_1})}, \qquad L_N^{(2)}(\xi; A_1) = 2A_1(1-\xi) \tag{9}$$

In order for $g''(\xi)$ to vanish at both ends of the interval $0 \leq \xi \leq 1$ it is sufficient to require the same of $L_N^{(2)}(\xi)$. One is then naturally led to consider a new choice for the generating function

$\phi(\xi)$ for which $\phi'(0) = \phi'(1) = 0$. For example, we can use

$$\phi_2(\xi) = 3\xi^2 - 2\xi^3 \quad \Rightarrow \quad L_N^{(2)}(\xi; A_2) = 6A_2\xi(1-\xi) \tag{10}$$

which should give a particularly advantageous distribution of grid points near the ends. Of course, the utility of this construction relative to equation (9) is predicated on the assumption that the constant A_2 will not greatly exceed the corresponding value of A_1 for a given set of mesh parameters. This assumption will be borne out by Table III, below.

With the aim of automatically matching higher derivatives at the junctions between patched stretching functions, one can generalize the above scheme to consider any non-decreasing, C^{n-1} generating function $\phi_n(\xi)$ that satisfies

$$\phi_n(0) = 0, \qquad \phi_n(1) = 1; \qquad \phi_n^{(i)}(0) = 0, \qquad \phi_n^{(i)}(1) = 0 \qquad (i = 1, \ldots, n-1). \tag{11}$$

The second through nth derivatives of the resulting stretching function $g_n(\xi)$ are then seen to vanish at both ends. No loss of generality ensues from setting the end values or from considering only monotonic functions $\phi_n(\xi)$. This case represents an elementary building block: the transition from the initial slope $g'(0)$ to the final slope $g'(1) = g'(0)e^A$. All other cases can be derived by splicing together such elementary pieces. Polynomials that satisfy the ascending conditions (11) with the smallest possible degree are given by Tables I and II; note that $\phi_n^{(n)}(0) \neq 0$ and $\phi_n^{(n)}(1) \neq 0$. Other functional forms could also be employed.

Stretching functions are typically used by specifying the initial slope $g'(0)$ (<1), which, for a given number N of grid intervals, gives the minimum mesh spacing inside the boundary layer.[3] (Without loss of generality one can consider the case $g'(1) > g'(0)$, because the transformation $\tilde{g}(\xi) = 1 - g(1-\xi)$ immediately yields the opposite case.) This leads to a non-linear equation for the constant A_n,

$$1 = g'(0) \int_0^1 e^{A_n \phi_n(t)}\, dt \tag{12}$$

We note that $A_n \to \infty$ as $g'(0) \to 0$; from the corresponding asymptotic behaviour of the integral[13] one can obtain an iteration scheme for calculating A_n numerically:

$$A_n = \ln\left\{\frac{A_n^{1/n}}{g'(0)F_n(A_n)}\right\} \tag{13}$$

Table I. Coefficients C_{nm} for the generating polynomials

$$\phi_n(\xi) = \xi^n \sum_{m=0}^{n-1} C_{nm}\xi^m$$

n \ m	0	1	2	3	4	5	6	7
2	3	−2						
3	10	−15	6					
4	35	−84	70	−20				
5	126	−420	540	−315	70			
6	462	−1980	3465	−3080	1386	−252		
7	1716	−9009	20020	−24024	16380	−6006	924	
8	6435	−40040	108108	−163800	150150	−83160	25740	−3432

Table II. Coefficients D_{nm} for an alternative, centered representation of the generating polynomials

$$\phi_n(\xi) = \tfrac{1}{2} + 4^{1-n} \sum_{m=1}^{n} D_{nm}(2\xi - 1)^{2m-1}$$

n \ m	1	2	3	4	5	6	7	8
2	3	−1						
3	15	−10	3					
4	70	−70	42	−10				
5	315	−420	378	−180	35			
6	1386	−2310	2772	−1980	770	−126		
7	6006	−12012	18018	−17160	10010	−3276	462	
8	25740	−60060	108108	−128700	100100	−49140	13860	−1716

with

$$F_n(A) = A^{1/n} e^{-A} \int_0^1 e^{A\phi(t)}\, dt \sim \frac{\Gamma(1/n)}{n} \left(\frac{n!}{(-1)^{n+1} \phi_n^{(n)}(1)} \right)^{1/n} \quad \text{as} \quad A \to \infty \tag{14}$$

For various values of the initial slope $g'(0)$, Table III gives the constants $A_1, \ldots, A_6$.

Aside from the need to evaluate polynomials of higher degree in the exponential, the computational labour of numerical integration required to implement the stretching functions (8), (11) is roughly equivalent, in nature and magnitude, to that for the usual erf-based function (9). For completeness we list the standard sinh-based and tanh-based stretching functions:[2,3]

$$\frac{\sinh(\alpha\xi)}{\sinh \alpha}, \qquad 1 - \frac{\tanh[\beta(1-\xi)]}{\tanh \beta} \tag{15}$$

For the fairly extreme case of initial slope $g'(0) = 10^{-6}$ (used as a test by Thompson and Mastin[3]), Figures 1 and 2 compare several of the stretching functions $g_n(\xi)$ with the hyperbolic sine, hyperbolic tangent and error function. Within the boundary layer ($\xi \approx 0$), small slope and curvature are desirable for close spacing and even distribution, respectively, of the grid points. In this regard the various stretching functions can be ranked as follows in order of increasing desirability: erf, tanh, sinh, g_2, g_3, g_4, g_5, g_6. With regard to close spacing of grid points (desired small slope) on the coarse end of the mesh, a similar ranking is as follows: sinh, tanh, g_2, g_3, g_4, erf, g_5, g_6. The trends with regard to sinh, tanh and erf have been noted previously.[2,3] (For convenience of uniformity, the calculations for the erf-based stretching function $g_1(\xi)$, equation (9), were carried out by the same scheme as for the higher $g_n(\xi)$). As the order n increases, the distribution $g_n(\xi)$ becomes straighter near the ends, with a concomitant increase in curvature in the middle, where the worst truncation error must then reside.

Figure 3 compares the truncation-error functions $L_N^{(2)}(\xi)$, $|L_N^{(3)}(\xi)|$, $L_S^{(2)}(\xi)$, $|L_S^{(3)}(\xi)|$ for sinh, tanh, erf and g_2. These are of roughly similar maximum magnitude in all cases, the more significant differences being the respective locations of the 'good' versus 'bad' zones of the various mappings. From Figure 4 we see that the main trend characterizing the ascending order of the $g_n(\xi)$ ($n = 1, \ldots, 6$) is a decrease in truncation error at the ends; in between we find a moderate increase in $L_N^{(2)}$ and $|L_N^{(3)}|$ (with concomitantly sharper peaks),

Table III. Constants $A_1, \ldots, A_6$ for various values of the initial slope $g'(0)$; see equations (12)–(14)

$g'(0)$	A_1	A_2	A_3	A_4	A_5	A_6
$5{\cdot}0\times10^{-1}$	0·979979	1·211755	1·190477	1·177637	1·168873	1·162425
$2{\cdot}0\times10^{-1}$	2·152225	2·513724	2·448968	2·411246	2·386035	2·367748
$1{\cdot}0\times10^{-1}$	2·984794	3·392840	3·298029	3·243605	3·207542	3·181532
$5{\cdot}0\times10^{-2}$	3·788419	4·223500	4·102437	4·033645	3·988328	3·955772
$2{\cdot}0\times10^{-2}$	4·821222	5·277117	5·126518	5·041761	4·986240	4·946501
$1{\cdot}0\times10^{-2}$	5·587004	6·052692	5·882933	5·787920	5·725882	5·681577
$5{\cdot}0\times10^{-3}$	6·343156	6·815802	6·629066	6·525027	6·457279	6·408983
$2{\cdot}0\times10^{-3}$	7·331617	7·810871	7·604370	7·489889	7·415561	7·362682
$1{\cdot}0\times10^{-3}$	8·072849	8·555881	8·336060	8·214578	8·135854	8·079922
$5{\cdot}0\times10^{-4}$	8·809635	9·295756	9·063759	8·935900	8·853184	8·794483
$2{\cdot}0\times10^{-4}$	9·778056	10·267529	10·020889	9·885391	9·797903	9·735899
$1{\cdot}0\times10^{-4}$	10·507155	10·998765	10·741970	10·601190	10·510410	10·446132
$5{\cdot}0\times10^{-5}$	11·233732	11·727220	11·460942	11·315242	11·221401	11·155011
$2{\cdot}0\times10^{-5}$	12·190906	12·686568	12·408644	12·256915	12·159329	12·090359
$1{\cdot}0\times10^{-5}$	12·912818	13·409938	13·123788	12·967809	12·867588	12·796804
$5{\cdot}0\times10^{-6}$	13·633106	14·131552	13·837617	13·677623	13·574914	13·502420
$2{\cdot}0\times10^{-6}$	14·583077	15·083110	14·779481	14·614496	14·508700	14·434085
$1{\cdot}0\times10^{-6}$	15·300227	15·801353	15·490795	15·322248	15·214251	15·138125

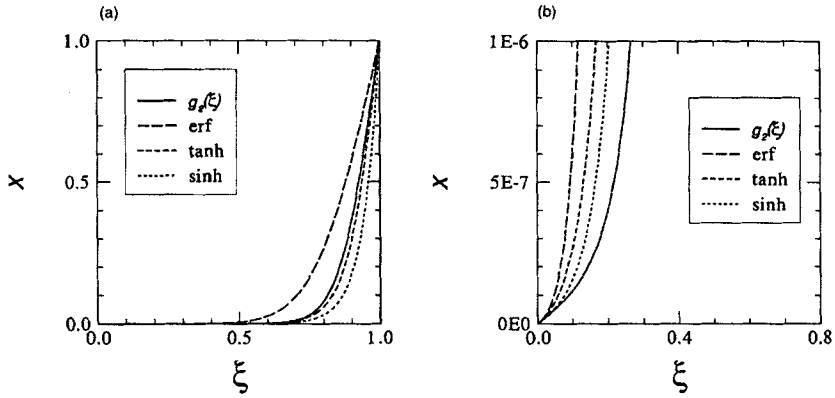

Figure 1. Stretching function $g_2(\xi)$ from equations (8), (10) compared with sinh, tanh and erf. All have the initial slope $g'(0) = 10^{-6}$: (a) overall distribution; (b) expanded view of boundary-layer region

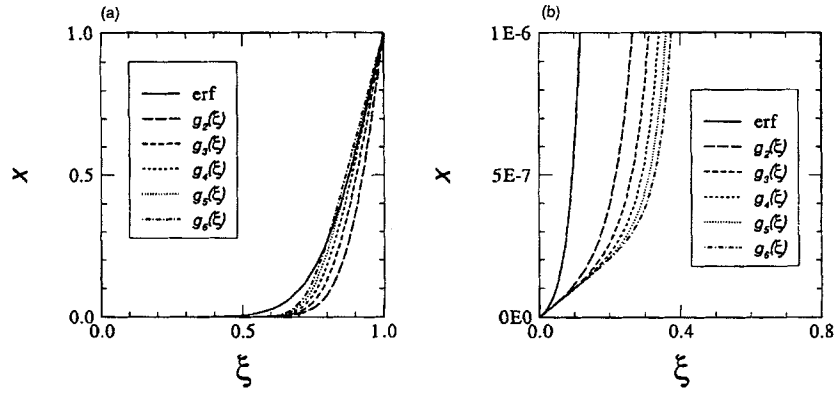

Figure 2. Ascending stretching functions $g_2(\xi), \ldots, g_6(\xi)$ from equations (8), (11). All have initial slope $g'(0) = 10^{-6}$: (a) overall distribution; (b) expanded view of boundary-layer region

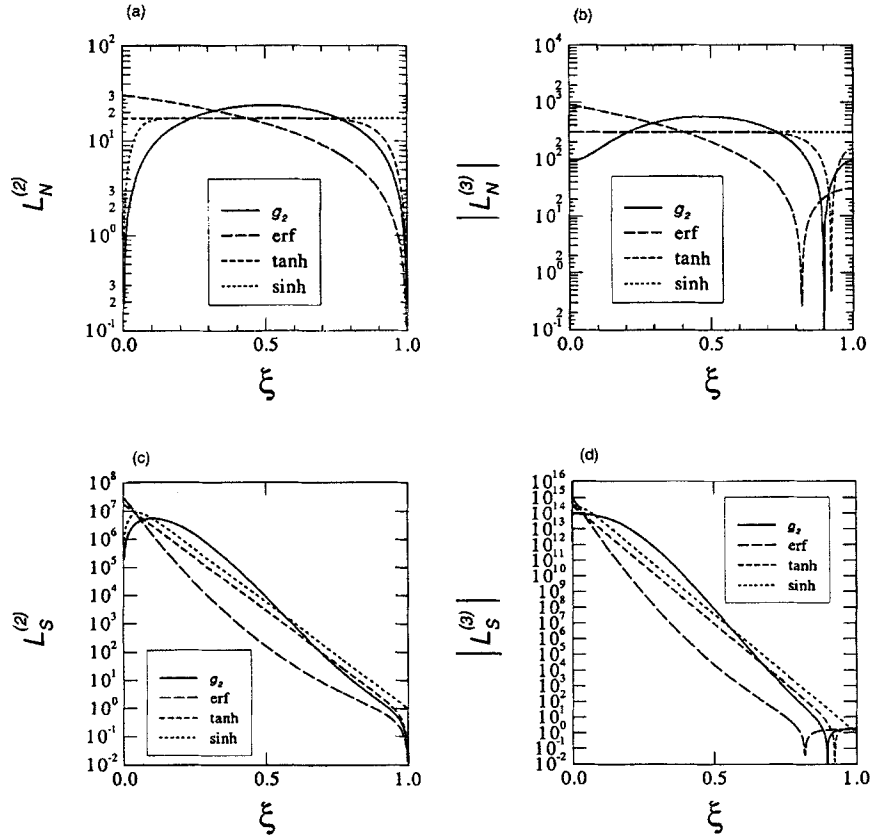

Figure 3. Truncation-error functions $L_N^{(2)}(\xi)$, $|L_N^{(3)}(\xi)|$, $L_S^{(2)}(\xi)$ and $|L_S^{(3)}(\xi)|$ for the stretching functions from Figure 1: $g_2(\xi)$, erf, tanh and sinh

but essentially no penalty with regard to $L_S^{(2)}$ and $L_S^{(3)}$. The price of truncation error payed in the middle (transition zone) is seen not to be excessive compared with sinh, tanh and erf – and well worth the advantage of C^n patching in troublesome regions of a domain, which is not possible with the simpler functions. The functions $L_N^{(3)}(\xi)$ and $L_S^{(3)}(\xi)$ are plotted in absolute value; where each quantity changes sign there is an infinite dip in the semilogarithmic graph. For sinh, tanh, erf and other stretching functions, similar graphs have been given previously.[3]

Although the above 'one-sided' stretching functions allow the slope $g'(\xi)$ to be prescribed only at one point (typically $\xi = 0$), an arbitrary grid spacing at both ends can be accommodated by a suitable adjustment of the number N of grid intervals. For various ratios of the minimum to maximum grid spacing, $g'(0)/g'(1)$, Table IV gives the (approximate) factor $g'(1)$ by which N must be increased relative to the base case (N_0) of a uniform mesh with the largest spacing:

$$\frac{N}{N_0} \approx \frac{g'(1)/(\Delta x)_{\max}}{1/(\Delta x)_{\max}} \tag{16}$$

This equation is exact only in the limit of infinitesimal spacing, $(\Delta x)_{\max} \to 0$ (i.e. $N_0 \to \infty$).

Table IV. Final slopes $g_1'(1), \ldots, g_6'(1)$ listed as functions of the refinement ratio $g'(0)/g'(1)$

$g'(0)/g'(1)$	$g_1'(1)$	$g_2'(1)$	$g_3'(1)$	$g_4'(1)$	$g_5'(1)$	$g_6'(1)$
$5{\cdot}0\times10^{-1}$	1·234529	1·373840	1·367273	1·363094	1·360144	1·357921
$2{\cdot}0\times10^{-1}$	1·543888	1·921568	1·876370	1·848437	1·829095	1·814723
$1{\cdot}0\times10^{-1}$	1·768609	2·343773	2·242172	2·181284	2·139956	2·109681
$5{\cdot}0\times10^{-2}$	1·981504	2·751772	2·573473	2·470115	2·401417	2·351827
$2{\cdot}0\times10^{-2}$	2·243368	3·253715	2·953218	2·786276	2·678174	2·601534
$1{\cdot}0\times10^{-2}$	2·427305	3·602242	3·200934	2·984394	2·846604	2·750069
$5{\cdot}0\times10^{-3}$	2·600257	3·925637	3·420800	3·155415	2·989120	2·873813
$2{\cdot}0\times10^{-3}$	2·814139	4·319711	3·677773	3·350298	3·148638	3·010423
$1{\cdot}0\times10^{-3}$	2·966273	4·596525	3·852228	3·479961	3·253300	3·099110
$5{\cdot}0\times10^{-4}$	3·111212	4·858018	4·013121	3·597913	3·347626	3·178487
$2{\cdot}0\times10^{-4}$	3·293209	5·183908	4·209008	3·739657	3·460002	3·272455
$1{\cdot}0\times10^{-4}$	3·424527	5·417713	4·346733	3·838216	3·537575	3·336982
$5{\cdot}0\times10^{-5}$	3·551018	5·642091	4·476908	3·930606	3·609906	3·396921
$2{\cdot}0\times10^{-5}$	3·711638	5·926074	4·639081	4·044735	3·698773	3·470278
$1{\cdot}0\times10^{-5}$	3·828676	6·132469	4·755260	4·125869	3·761638	3·521994
$5{\cdot}0\times10^{-6}$	3·942243	6·332393	4·866525	4·203103	3·821254	3·570904
$2{\cdot}0\times10^{-6}$	4·087533	6·587741	5·006914	4·299926	3·895683	3·631792
$1{\cdot}0\times10^{-6}$	4·194098	6·774777	5·108578	4·369619	3·949053	3·675336

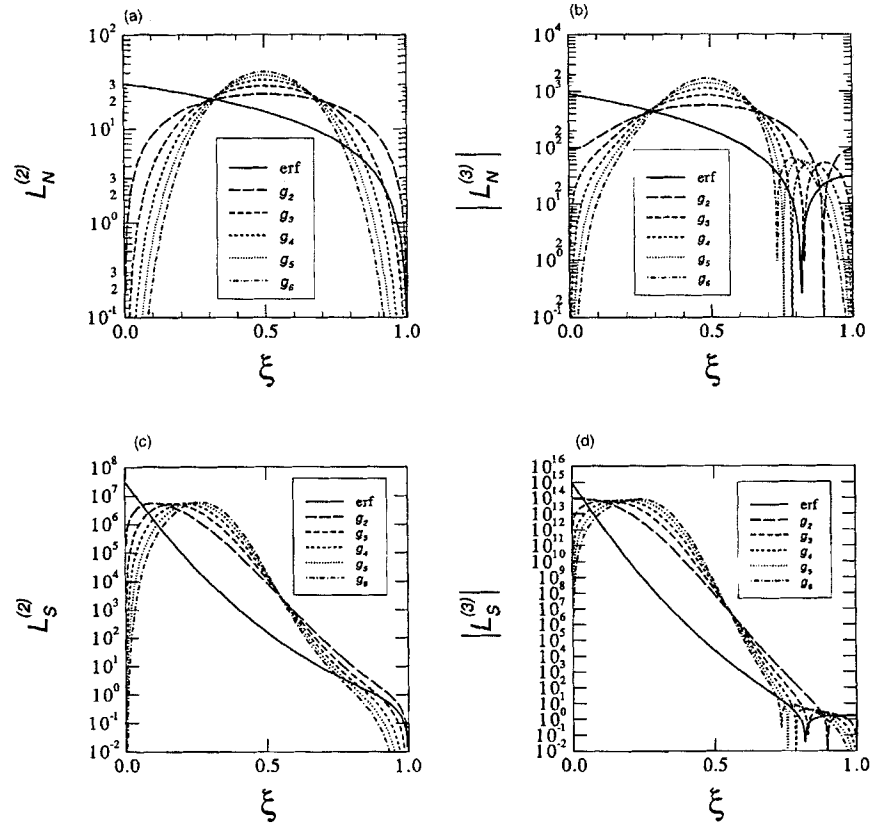

Figure 4. Truncation-error functions $L_N^{(2)}(\xi)$, $|L_N^{(3)}(\xi)|$, $L_S^{(2)}(\xi)$ and $|L_S^{(3)}(\xi)|$ for the stretching functions from Figure 2: $g_2(\xi), \ldots, g_6(\xi)$

STRETCHING FUNCTIONS BASED UPON $L_S^{(2)}$

Working backwards from the truncation-error function $L_S^{(2)}$, equation (6), one observes that the functional form

$$h(\xi; B) = h'(0) \int_0^{\xi} \frac{dt}{1 - B\phi(t)} \quad \Rightarrow \quad L_S^{(2)}(\xi; B) = B\phi'(\xi)/h'(0) \tag{17}$$

Here the same generating functions from equation (11) yield the desired end conditions $h_n^{(i)}(0) = h_n^{(i)}(1) = 0$ $(i = 2, \ldots, n)$ for C^n matching as before. Given the initial slope $h'(0)$, the value of the constant B for which $h(1) = 1$ can be determined numerically from the iteration scheme

$$B = 1 - h'(0)F(B) \tag{18}$$

with

$$F(B) = (1 - B) \int_0^1 \frac{dt}{1 - B\phi(t)} \to 0 \quad \text{as} \quad B \to 1 \tag{19}$$

Values of $(1 - B_n)$ for various initial slopes $h'(0)$ are listed in Table V.

Figure 5 compares the $L_N^{(2)}$-based stretching functions $g_2(\xi)$, $g_6(\xi)$ for $g'(0) = 10^{-6}$ with their $L_S^{(2)}$-based counterparts $h_2(\xi)$, $h_6(\xi)$, equations (11), (17). In each case the terminal slope $h_n'(1)$ matches the corresponding value of $g_n'(1)$, so that the outer (i.e. widest) mesh spacing is the same. With reference to equation (16) it follows that, for the same number of mesh points, the more slowly varying h stretching functions are therefore capable only of much poorer refinement in the boundary layer (given by the initial slopes): $h'(0) = 0{\cdot}1484$, $h_6'(0) = 0{\cdot}09041$. A related conclusion follows from comparing Tables IV and VI: for the same refinement ratio $h'(0)/h'(1) \approx (\Delta x)_{\min}/(\Delta x)_{\max}$, each of the $h_n(\xi)$ stretching functions

Table V. Constants $(1 - B_2), \ldots, (1 - B_6)$ for various values of the initial slope $h'(0)$; see equations (18) and (19)

$h'(0)$	$1 - B_2$	$1 - B_3$	$1 - B_4$	$1 - B_5$	$1 - B_6$
$5{\cdot}0 \times 10^{-1}$	$2{\cdot}466855 \times 10^{-1}$	$2{\cdot}650575 \times 10^{-1}$	$2{\cdot}755734 \times 10^{-1}$	$2{\cdot}825337 \times 10^{-1}$	$2{\cdot}875514 \times 10^{-1}$
$2{\cdot}0 \times 10^{-1}$	$3{\cdot}765648 \times 10^{-2}$	$5{\cdot}268787 \times 10^{-2}$	$6{\cdot}151172 \times 10^{-2}$	$6{\cdot}741055 \times 10^{-2}$	$7{\cdot}168522 \times 10^{-2}$
$1{\cdot}0 \times 10^{-1}$	$9{\cdot}045535 \times 10^{-3}$	$1{\cdot}664602 \times 10^{-2}$	$2{\cdot}157771 \times 10^{-2}$	$2{\cdot}501665 \times 10^{-2}$	$2{\cdot}756799 \times 10^{-2}$
$5{\cdot}0 \times 10^{-2}$	$2{\cdot}188032 \times 10^{-3}$	$5{\cdot}464304 \times 10^{-3}$	$7{\cdot}898491 \times 10^{-3}$	$9{\cdot}692604 \times 10^{-3}$	$1{\cdot}106454 \times 10^{-2}$
$2{\cdot}0 \times 10^{-2}$	$3{\cdot}399517 \times 10^{-4}$	$1{\cdot}300538 \times 10^{-3}$	$2{\cdot}174977 \times 10^{-3}$	$2{\cdot}875254 \times 10^{-3}$	$3{\cdot}435303 \times 10^{-3}$
$1{\cdot}0 \times 10^{-2}$	$8{\cdot}385998 \times 10^{-5}$	$4{\cdot}468398 \times 10^{-4}$	$8{\cdot}347198 \times 10^{-4}$	$1{\cdot}166728 \times 10^{-3}$	$1{\cdot}441940 \times 10^{-3}$
$5{\cdot}0 \times 10^{-3}$	$2{\cdot}079403 \times 10^{-5}$	$1{\cdot}549798 \times 10^{-4}$	$3{\cdot}234517 \times 10^{-4}$	$4{\cdot}778662 \times 10^{-4}$	$6{\cdot}106670 \times 10^{-4}$
$2{\cdot}0 \times 10^{-3}$	$3{\cdot}307364 \times 10^{-6}$	$3{\cdot}857806 \times 10^{-5}$	$9{\cdot}326385 \times 10^{-5}$	$1{\cdot}482277 \times 10^{-4}$	$1{\cdot}979103 \times 10^{-4}$
$1{\cdot}0 \times 10^{-3}$	$8{\cdot}249043 \times 10^{-7}$	$1{\cdot}353336 \times 10^{-5}$	$3{\cdot}658150 \times 10^{-5}$	$6{\cdot}144228 \times 10^{-5}$	$8{\cdot}479134 \times 10^{-5}$
$5{\cdot}0 \times 10^{-4}$	$2{\cdot}059528 \times 10^{-7}$	$4{\cdot}759193 \times 10^{-6}$	$1{\cdot}438987 \times 10^{-5}$	$2{\cdot}554396 \times 10^{-5}$	$3{\cdot}643360 \times 10^{-5}$
$2{\cdot}0 \times 10^{-4}$	$3{\cdot}292286 \times 10^{-8}$	$1{\cdot}198427 \times 10^{-6}$	$4{\cdot}204927 \times 10^{-6}$	$8{\cdot}032332 \times 10^{-6}$	$1{\cdot}196768 \times 10^{-5}$
$1{\cdot}0 \times 10^{-4}$	$8{\cdot}227945 \times 10^{-9}$	$4{\cdot}227407 \times 10^{-7}$	$1{\cdot}660787 \times 10^{-6}$	$3{\cdot}354101 \times 10^{-6}$	$5{\cdot}165458 \times 10^{-6}$
$5{\cdot}0 \times 10^{-5}$	$2{\cdot}056609 \times 10^{-9}$	$1{\cdot}492233 \times 10^{-7}$	$6{\cdot}566474 \times 10^{-7}$	$1{\cdot}402334 \times 10^{-6}$	$2{\cdot}232444 \times 10^{-6}$
$2{\cdot}0 \times 10^{-5}$	$3{\cdot}290178 \times 10^{-10}$	$3{\cdot}769807 \times 10^{-8}$	$1{\cdot}928180 \times 10^{-7}$	$4{\cdot}434588 \times 10^{-7}$	$7{\cdot}376837 \times 10^{-7}$
$1{\cdot}0 \times 10^{-5}$	$8{\cdot}225087 \times 10^{-11}$	$1{\cdot}331897 \times 10^{-8}$	$7{\cdot}635979 \times 10^{-8}$	$1{\cdot}857831 \times 10^{-7}$	$3{\cdot}195279 \times 10^{-7}$

Table VI. Final slopes $h_2'(1), \ldots, h_6'(1)$ listed as functions of the refinement ratio $h'(0)/h'(1)$

$h'(0)/h'(1)$	$h_2'(1)$	$h_3'(1)$	$h_4'(1)$	$h_5'(1)$	$h_6'(1)$
$5{\cdot}0\times10^{-1}$	$1{\cdot}416614\times10^{0}$	$1{\cdot}402896\times10^{0}$	$1{\cdot}394198\times10^{0}$	$1{\cdot}388075\times10^{0}$	$1{\cdot}383472\times10^{0}$
$2{\cdot}0\times10^{-1}$	$2{\cdot}255592\times10^{0}$	$2{\cdot}142514\times10^{0}$	$2{\cdot}074023\times10^{0}$	$2{\cdot}027361\times10^{0}$	$1{\cdot}993136\times10^{0}$
$1{\cdot}0\times10^{-1}$	$3{\cdot}215606\times10^{0}$	$2{\cdot}901627\times10^{0}$	$2{\cdot}721697\times10^{0}$	$2{\cdot}603717\times10^{0}$	$2{\cdot}519579\times10^{0}$
$5{\cdot}0\times10^{-2}$	$4{\cdot}590580\times10^{0}$	$3{\cdot}878425\times10^{0}$	$3{\cdot}497707\times10^{0}$	$3{\cdot}259367\times10^{0}$	$3{\cdot}094940\times10^{0}$
$2{\cdot}0\times10^{-2}$	$7{\cdot}354242\times10^{0}$	$5{\cdot}593924\times10^{0}$	$4{\cdot}748870\times10^{0}$	$4{\cdot}254859\times10^{0}$	$3{\cdot}929862\times10^{0}$
$1{\cdot}0\times10^{-2}$	$1{\cdot}050044\times10^{1}$	$7{\cdot}300043\times10^{0}$	$5{\cdot}895112\times10^{0}$	$5{\cdot}117267\times10^{0}$	$4{\cdot}623949\times10^{0}$
$5{\cdot}0\times10^{-3}$	$1{\cdot}498043\times10^{1}$	$9{\cdot}455141\times10^{0}$	$7{\cdot}246682\times10^{0}$	$6{\cdot}089334\times10^{0}$	$5{\cdot}381433\times10^{0}$
$2{\cdot}0\times10^{-3}$	$2{\cdot}392291\times10^{1}$	$1{\cdot}318973\times10^{1}$	$9{\cdot}414372\times10^{0}$	$7{\cdot}573659\times10^{0}$	$6{\cdot}499043\times10^{0}$
$1{\cdot}0\times10^{-3}$	$3{\cdot}404311\times10^{1}$	$1{\cdot}687704\times10^{1}$	$1{\cdot}140401\times10^{1}$	$8{\cdot}875362\times10^{0}$	$7{\cdot}448763\times10^{0}$
$5{\cdot}0\times10^{-4}$	$4{\cdot}839252\times10^{1}$	$2{\cdot}152033\times10^{1}$	$1{\cdot}375965\times10^{1}$	$1{\cdot}035923\times10^{1}$	$8{\cdot}503765\times10^{0}$
$2{\cdot}0\times10^{-4}$	$7{\cdot}692485\times10^{1}$	$2{\cdot}955487\times10^{1}$	$1{\cdot}755712\times10^{1}$	$1{\cdot}265059\times10^{1}$	$1{\cdot}008608\times10^{1}$
$1{\cdot}0\times10^{-4}$	$1{\cdot}091261\times10^{2}$	$3{\cdot}748503\times10^{1}$	$2{\cdot}105790\times10^{1}$	$1{\cdot}467706\times10^{1}$	$1{\cdot}144673\times10^{1}$
$5{\cdot}0\times10^{-5}$	$1{\cdot}547047\times10^{2}$	$4{\cdot}747254\times10^{1}$	$2{\cdot}521493\times10^{1}$	$1{\cdot}699930\times10^{1}$	$1{\cdot}296905\times10^{1}$
$2{\cdot}0\times10^{-5}$	$2{\cdot}452016\times10^{2}$	$6{\cdot}476013\times10^{1}$	$3{\cdot}193332\times10^{1}$	$2{\cdot}060057\times10^{1}$	$1{\cdot}526526\times10^{1}$
$1{\cdot}0\times10^{-5}$	$3{\cdot}472361\times10^{2}$	$8{\cdot}182877\times10^{1}$	$3{\cdot}813765\times10^{1}$	$2{\cdot}379462\times10^{1}$	$1{\cdot}724724\times10^{1}$
$5{\cdot}0\times10^{-6}$	$4{\cdot}915740\times10^{2}$	$1{\cdot}033309\times10^{2}$	$4{\cdot}551269\times10^{1}$	$2{\cdot}746094\times10^{1}$	$1{\cdot}946955\times10^{1}$
$2{\cdot}0\times10^{-6}$	$7{\cdot}780224\times10^{2}$	$1{\cdot}405577\times10^{2}$	$5{\cdot}744167\times10^{1}$	$3{\cdot}315392\times10^{1}$	$2{\cdot}282734\times10^{1}$
$1{\cdot}0\times10^{-6}$	$1{\cdot}100889\times10^{3}$	$1{\cdot}773189\times10^{2}$	$6{\cdot}846382\times10^{1}$	$3{\cdot}820747\times10^{1}$	$2{\cdot}572895\times10^{1}$

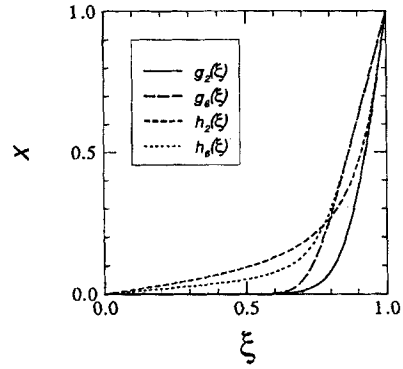

Figure 5. Comparison of the $L_N^{(2)}$-based stretching functions $g_2(\xi)$, $g_6(\xi)$ from Figure 2 ($g'(0) = 10^{-6}$) with the $L_S^{(2)}$-based functions $h_2(\xi)$, $h_6(\xi)$, Equations (11), (17). In each case ($n = 2, 6$) the terminal slope $h_n'(1)$ matches $g_n'(1)$, so that the outer mesh spacing would be the same (for the same number of nodes)

requires more mesh points than the corresponding function $g_n(\xi)$ – the difference being very dramatic at the smallest refinement ratios. This is the price of the dramatically smaller truncation-error functions $L_S^{(2)}(\xi)$ and $L_S^{(3)}(\xi)$ shown in Figure 6. The functions $L_N^{(2)}(\xi)$ and $L_N^{(3)}(\xi)$ for the two types of stretching functions are, however, closer in magnitude. Through analogous comparisons involving prescribed *initial* slope, Thompson and Mastin[3] concluded that the more restrictive concept of order with fixed number of grid points will generally be impractical to take advantage of for wide variations in mesh density. For less extreme cases the h functions would be more useful.

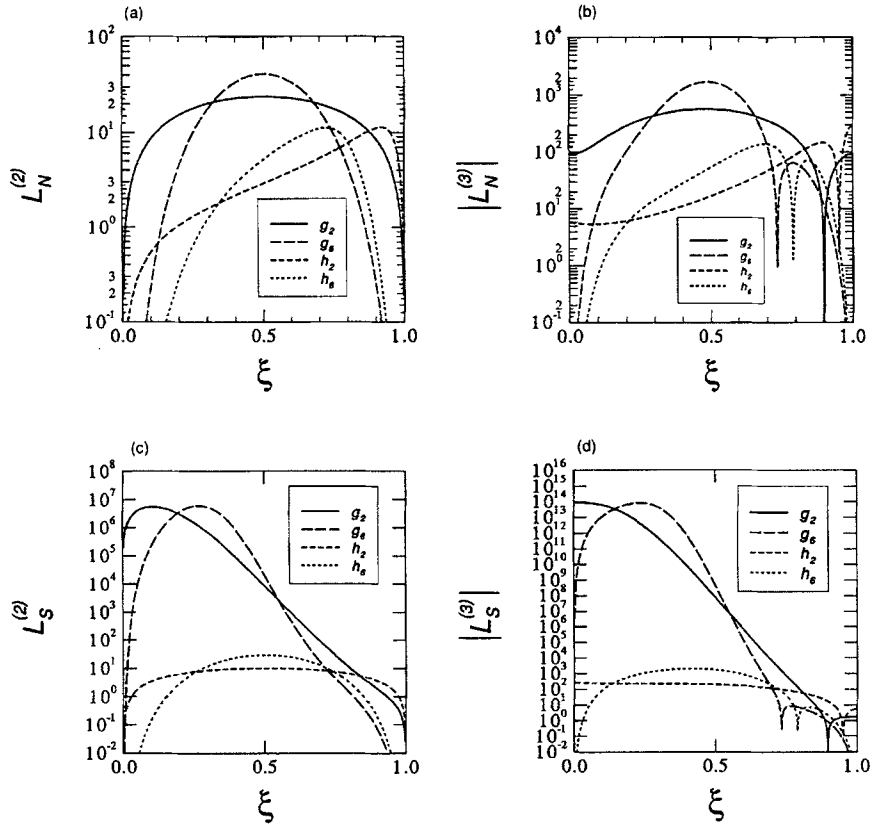

Figure 6. Truncation-error functions $L_N^{(2)}(\xi)$, $|L_N^{(3)}(\xi)|$, $L_S^{(2)}(\xi)$ and $|L_S^{(3)}(\xi)|$ for the stretching functions from Figure 5: $g_2(\xi)$, $g_6(\xi)$, $h_2(\xi)$ and $h_6(\xi)$

TWO-SIDED STRETCHING FUNCTIONS

In order to prescribe both the minimum and maximum grid spacing without tying up the degree of freedom associated with the total number N of grid intervals, one needs a 'two-sided' stretching function that allows the slopes at both ends to be specified arbitrarily. Vinokur[9] has given a method of construction of two-sided stretching functions from the more elementary one-sided functions; such prescriptions are also reviewed in Chapter VIII of the monograph by Thompson, Warsi and Mastin.[2] Unfortunately, this general type of scheme relies on a transformation,

$$G(\xi) = \frac{g(\xi)}{C + (1 - C)g(\xi)} \tag{20}$$

that ruins the simple relationship, (8) or (17), between the generating function $\phi(\xi)$ and the associated truncation-error function. As an alternative, we consider here the construction of two-sided stretching functions by patching together two of the one-sided functions. (As before, the subsequent derivation can, without loss of generality, be confined to the case $G'(1) \leqslant G'(0)$;

$$\tilde{G}(\xi) = 1 - G(1 - \xi) \tag{21}$$

immediately yields the opposite case.)

For the $L_N^{(2)}$-based stretching functions, equation (8), the process of matching function values and slopes at the arbitrary junction $\xi = \xi^*$ leads to the formula.

$$G(\xi) = \begin{cases} \xi^* g(\xi/\xi^*; A), & 0 \leqslant \xi \leqslant \xi^* \\ \xi^* g(1; A) + e^A(1-\xi^*) g\left(\dfrac{\xi-\xi^*}{1-\xi^*}; \ln\left[\dfrac{G'(1)}{G'(0)}\right] - A\right), & \xi^* \leqslant \xi \leqslant 1 \end{cases} \tag{22}$$

The two-sided stretching function $G_n(\xi)$ is generated using $\phi(t) \equiv \phi_n(t)$. Continuity of the first n derivatives of $G_n(\xi)$ then follows automatically from (11). In (22) we have, for the sake of brevity, omitted the subscript n, and we continue to do so throughout this Section, except for the last paragraph.

The boundary condition $G(1) = 1$ leads to a relationship between the two free shape parameters ξ^* and A. If one prescribes the value of A arbitrarily, then the matching point ξ^* is determined:

$$\xi^* = \frac{1 - e^A g(1; \ln[G'(1)/G'(0)] - A)}{g(1; A) - e^A g(1; \ln[G'(1)/G'(0)]1 - A)} \tag{23}$$

The particular choice $A = \ln \sqrt{[G'(1)/G'(0)]}$ leads to the formula

$$\xi^* = \frac{1 - \{Q(\sqrt{[G'(1)/G'(0)]})\sqrt{[G'(0)G'(1)]}\}^{-1}}{1 - \sqrt{[G'(0)/G'(1)]}}, \qquad Q(X) \overset{\text{def}}{=} \int_0^1 X^{\phi(t)}\, dt \tag{24}$$

Because we must have $0 < \xi^* < 1$, there arise upper and lower bounds on the ratio of the final to initial slope:

$$J^2 < G'(1)/G'(0) < e^{2A} \tag{25}$$

with A listed as a function of the initial slope in Table III [with $g'(0)$ in place of $G'(0)$], as given by equations (12)–(14), and $J = J[G'(0)]$ determined from the non-linear equation

$$JQ(J) = [G'(0)]^{-1} \tag{26}$$

An analogous scheme for the $L_S^{(2)}$-based stretching functions, equation (17), yields

$$H(\xi) = \begin{cases} \xi^* h(\xi/\xi^*; B), & 0 \leqslant \xi \leqslant \xi^* \\ \xi^* h(1; B) + \dfrac{1-\xi^*}{1-B} h\left(\dfrac{\xi-\xi^*}{1-\xi^*}; 1 - \dfrac{H'(0)/H'(1)}{1-B}\right), & \xi^* \leqslant \xi \leqslant 1 \end{cases} \tag{27}$$

If we prescribe the value of B, then the boundary condition $H(1) = 1$ yields

$$\xi^* = \frac{(1-B) - h\left(1; 1 - \dfrac{H'(0)/H'(1)}{1-B}\right)}{(1-B)h(1; B) - h\left(1; 1 - \dfrac{H'(0)/H'(1)}{1-B}\right)} \tag{28}$$

For the special choice $B = 1 - \sqrt{[H'(0)/H'(1)]}$ we find

$$\xi^* = \frac{1 - \{R(\sqrt{[H'(0)/H'(1)]})\sqrt{[H'(0)H'(1)]}\}^{-1}}{1 - \sqrt{[H'(0)/H'(1)]}}, \qquad R(X) \overset{\text{def}}{=} \int_0^1 \frac{dt}{1 - (1-X)\phi(t)} \tag{29}$$

The ratio of final to initial slope is bounded as follows:

$$K^2 < H'(1)/H'(0) < (1-B)^{-2} \tag{30}$$

with $1 - B$ listed as a function of the initial slope in Table IV [with $h'(0)$ in place of $H'(0)$], as given by equations (18) and (19), and $K = K[H'(0)]$ determined from the nonlinear equation

$$KR(1/K) = [H'(0)]^{-1} \tag{31}$$

It is interesting to note that (22) and (27) can be regarded as resulting from formulas similar to (8) and (17), respectively, if we use the appropriate, two-piece generating functions $\psi_G(t)$ and $\psi_H(t)$ in place of $\phi(t)$:

$$G(\xi) = G'(0)\int_0^{\xi} e^{\psi_G(t)}\,dt, \qquad H(\xi) = H'(0)\int_0^{\xi} \frac{dt}{1-\psi_H(t)} \tag{32}$$

with

$$\psi_G(\xi) = \begin{cases} A\phi\left(\dfrac{\xi}{\xi^*}\right), & 0 \leq \xi \leq \xi^* \\ A + \left\{\ln\left[\dfrac{G'(1)}{G'(0)}\right] - A\right\}\phi\left(\dfrac{\xi-\xi^*}{1-\xi^*}\right), & \xi^* \leq \xi \leq 1 \end{cases} \tag{33}$$

and

$$\psi_H(\xi) = \begin{cases} B\phi\left(\dfrac{\xi}{\xi^*}\right), & 0 \leq \xi \leq \xi^* \\ B + \left[1 - B - \dfrac{H'(0)}{H'(1)}\right]\phi\left(\dfrac{\xi-\xi^*}{1-\xi^*}\right), & \xi^* \leq \xi \leq 1 \end{cases} \tag{34}$$

These forms, each of which has the basic appearance of two rounded stairs, expose an analogy with the global approach of Oh,[12] which is also reviewed by Thompson *et al.*[1] The global generating function of Oh [renamed here $\Psi(\xi)$] consisted of a suitable superposition of complementary error functions, and incorporated multiple transitions between fine and coarse zones of a grid, with regularity C^∞. However, the resulting global stretching function was simply obtained as the antiderivative of $\Psi(\xi)$, and the truncation error was not treated by Oh. We note here that a global generating function like $\Psi(\xi)$ could be reused in new ways in (32) to obtain new classes of C^∞ stretching functions that are formulated with direct reference to the pertinent truncation-error criteria; cf. (8) and (17).

If one is satisfied with C^n regularity of a composite stretching function, then this can be spliced together from two-sided pieces of the form $G_n(\xi)$ and/or $H_n(\xi)$. (There is no reason why the two types of functions cannot be mixed together.) In this way one avoids the linear algebraic system that must be solved for the relevant shape parameters in the global stretching function developed by Oh.[12,1]

CONCLUDING REMARKS

The one-sided (g_n, h_n) and two-sided (G_n, H_n) stretching functions developed in this paper have two particularly desirable features for generating composite grids for finite-difference calculations. Firstly, the distribution of nodes can be arranged to be advantageous with respect to either conception of truncation order (fixed relative distribution against fixed number of points). Secondly, C^n regularity of the composite stretching function requires matching of only

the function values and slopes on either side of each junction, because the higher derivatives (through order n) vanish at these points, and so match trivially.

Composite grids based upon some of the one-sided stretching functions described above have been employed in the finite-difference numerical solution of two-dimensional, steady-state (elliptic) advection–diffusion problems in connection with antipolarization dialysis.[14] (In that case the splicing procedure was somewhat related to the general approach embodied in (32)–(34). Once the desired mesh parameters were chosen, the number of nodes was determined, and could not be specified independently.) It is planned by the author to present calculations using the two-sided stretching functions in a subsequent paper. Finally, we remark that it would be interesting to investigate the applicability of the approach used here to multidimensional stretching functions, which have recently been developed.[11]

ACKNOWLEDGEMENTS

A kind letter from Prof. C. Wayne Mastin provided valuable perspective on the motivation and applications of smoothly patched grids and on related elements of interpolation, for which the author would like to express his gratitude. Thanks are also due to Ms. Shan Zhuge, who assisted in surveying the literature. Financial support from the National Science Foundation (grant no. CTS–9210277) is gratefully acknowledged.

REFERENCES

1. J. F. Thompson, Z. U. A. Warsi and C. W. Mastin, 'Boundary-fitted coordinate systems for numerical solution of partial differential equations-A review', *J. Comput. Phys.*, **47**, 1–108 (1982).
2. J. F. Thompson, Z. U. A. Warsi and C. W. Mastin, *Numerical Grid Generation. Foundations and Applications*, North-Holland (Elsevier), New York, 1985.
3. J. F. Thompson and C. W. Mastin, 'Order of difference expressions in curvilinear coordinate systems', *J. Fluids Eng.*, **107**, 241–250 (1985).
4. T. I.-P. Shih, R. T. Bailey, H. L. Nguyen and R. J. Roelke, 'Algebraic grid generation for complex geometries', *Int. j. numer. methods fluids*, **13**, 1–31 (1991).
5. G. S. Dietachmayer and K. K. Droegemeier, 'Application of continuous dynamic grid adaptation techniques to meteorological modeling. Part I: Basic formulation and accuracy', *Mon. Weather Rev.*, **120**, 1675–1706 (1992); G. S. Dietachmayer '... Part II: Efficiency', *ibid.*, 1707–1722 (1992).
6. H. J. Kim and J. F. Thompson, 'Three-dimensional adaptive grid generation on a composite-block grid', *AIAA J.*, **28**, 470–477 (1990).
7. J. U. Brackbill and J. Saltzman, 'An adaptive computation mesh for the solution of singular perturbation problems', in *Numerical Grid Generation Techniques*, NASA Conference Publication 2166, 1980, pp. 193–196, N81–14701.
8. J. D. Hoffman, 'Relationship between the truncation errors of centered finite-difference approximations on uniform and nonuniform meshes', *J. Comput. Phys.*, **46**, 469–474 (1982).
9. M. Vinokur, 'On one-dimensional stretching functions for finite-difference calculations', *J. Comput. Phys.*, **50**, 215–234 (1983); see also NASA CR 3313 (1980).
10. P. R. Eiseman, 'Coordinate generation with precise controls over mesh properties', *J. Comput. Phys.*, **47**, 331–351 (1982); 'High level continuity for coordinate generation with precise controls', *ibid.*, 352–374 (1982).
11. E. Steinthorsson, T. I.-P. Shih and R. J. Roelke, 'Enhancing control of grid distribution in algebraic grid generation', *Int. j. numer. methods fluids*, **15**, 297–311 (1992).
12. Y. H. Oh, 'An analytical transformation technique for generating uniformly spaced computational mesh', in *Numerical Grid Generation Techniques*, NASA Conference Publication 2166, 1980, pp. 385–398, N81–14717.
13. C. M. Bender and S. A. Orszag, *Advanced Mathematical Methods for Scientists and Engineers*, McGraw-Hill, New York, 1978, Section 6·4.
14. L. C. Nitsche and S. Zhuge, 'Hydrodynamics and selectivity of antipolarization dialysis', *Chem. Eng. Sci.*, **50**, 2731–2746 (1995).